# THE MEASURED MOTIONS INSIDE EQUATORIAL PLASMA BUBBLES

W. B. Hanson
Center for Space Sciences
P.O. Box 688
The University of Texas at Dallas
Richardson, TX 75080

D. K. Bamgboye
Physics Department
University of Ilorin
Ilorin, Nigeria

A preliminary study of the vertical and north-south horizontal ion motions in plasma bubbles in the near-equatorial ionosphere utilizing drift meter data from Atmosphere Explorer E is presented. High-resolution data show that the vertical ion velocity in some bubbles increases approximately linearly with $(N_0-N)/N$, where $N_0$ is the background ion concentration and N is the bubble ion concentration. At sufficiently large $N_0/N$ the vertical ion velocity saturates, but often at a value substantially larger than the ratio of the gravitational acceleration to the ion neutral collision frequency ($g/\nu_{in}$), which is the nominal collision-dominated velocity limit for cylindrical bubbles. These larger than nominal velocities may result from background eastward electric fields and/or from a vertically elongated bubble cross section. The unanticipated observation that large poleward horizontal drifts accompany these vertical drifts seems to follow naturally from a redistribution of plasma along flux tubes as the plasma convects from the bottomside of the F region to high altitudes.

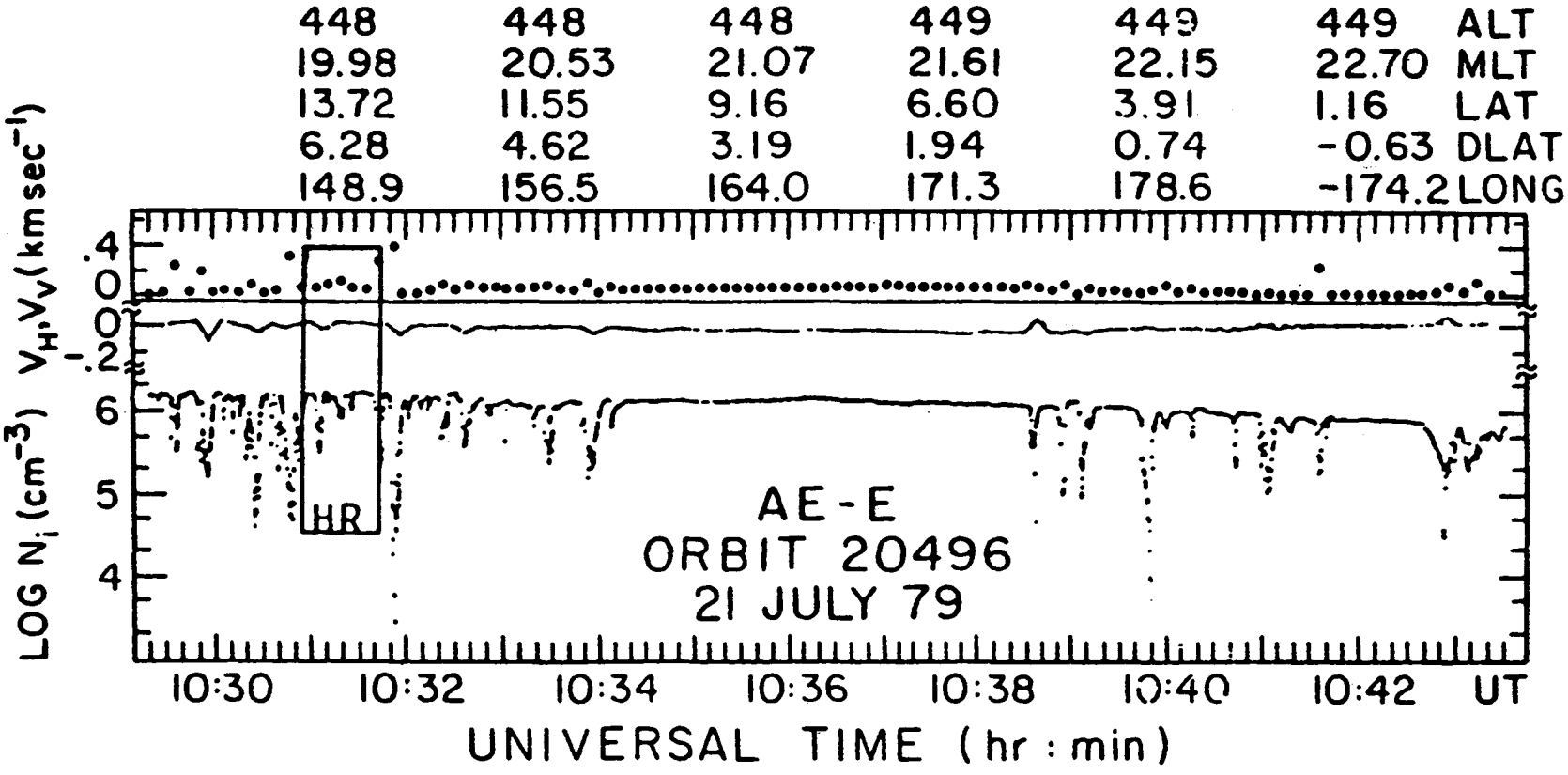


Figure 1. Ion number density and drift data (absolute points only) from the ion drift meter showing (in the lower trace) the density depletions (bubbles) and their horizontal (middle trace) and vertical (solid dots) velocities. The horizontal velocities are in a direction normal to the satellite velocity vector. The data are from AE-E orbit 20496 on July 21, 1979, when Ap = 7, Kp = 2, and $F_{10.7}$ = 144.

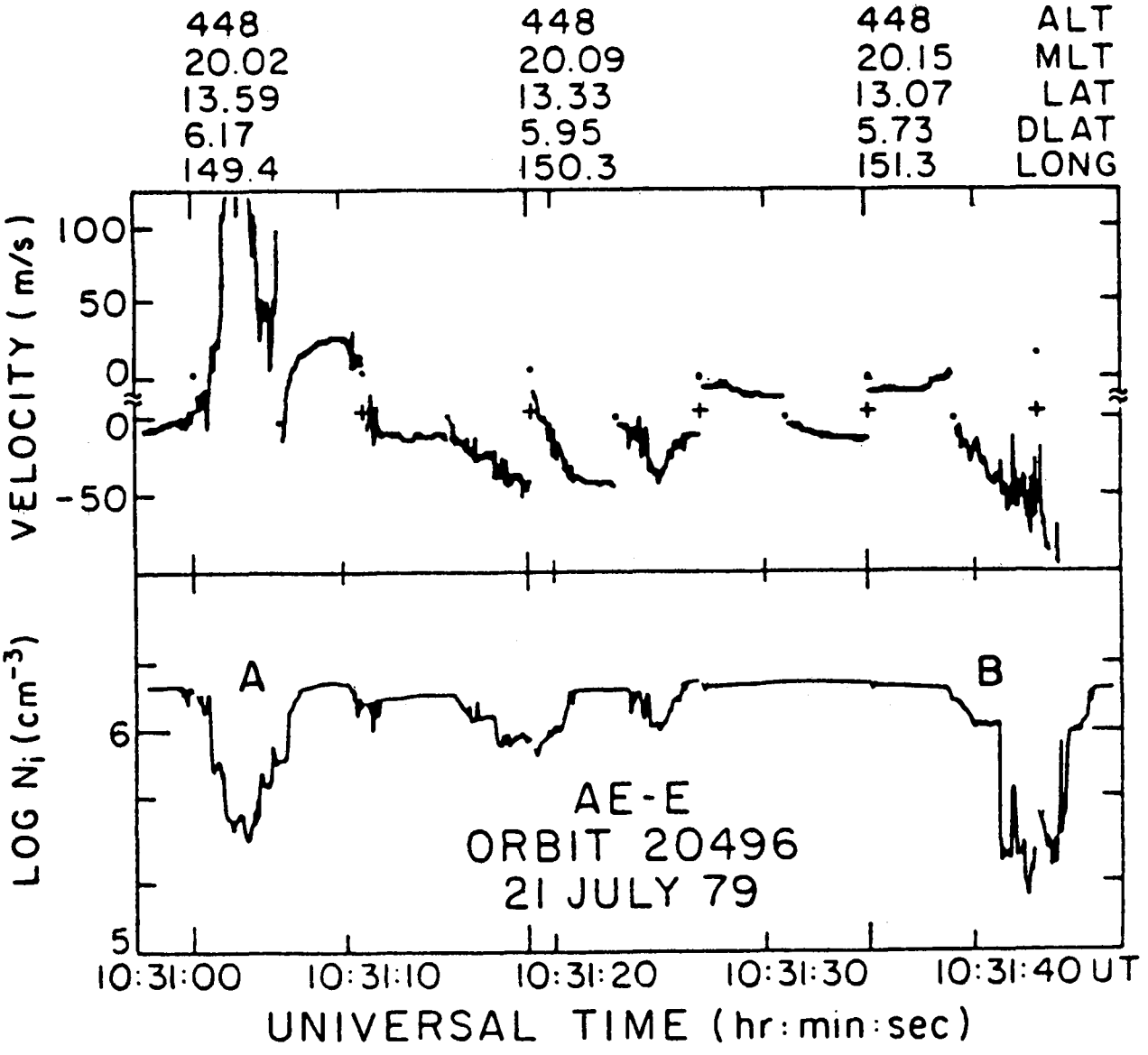


Figure 2. High-resolution version of the portion of Figure 1 marked HR. Note how depletions and velocities that are barely visible in Figure 1 can be quite clearly identified and measured in this format. Alternate 4-s segments of pitch (vertical) and yaw (horizontally) velocity data are shown in the upper trace.

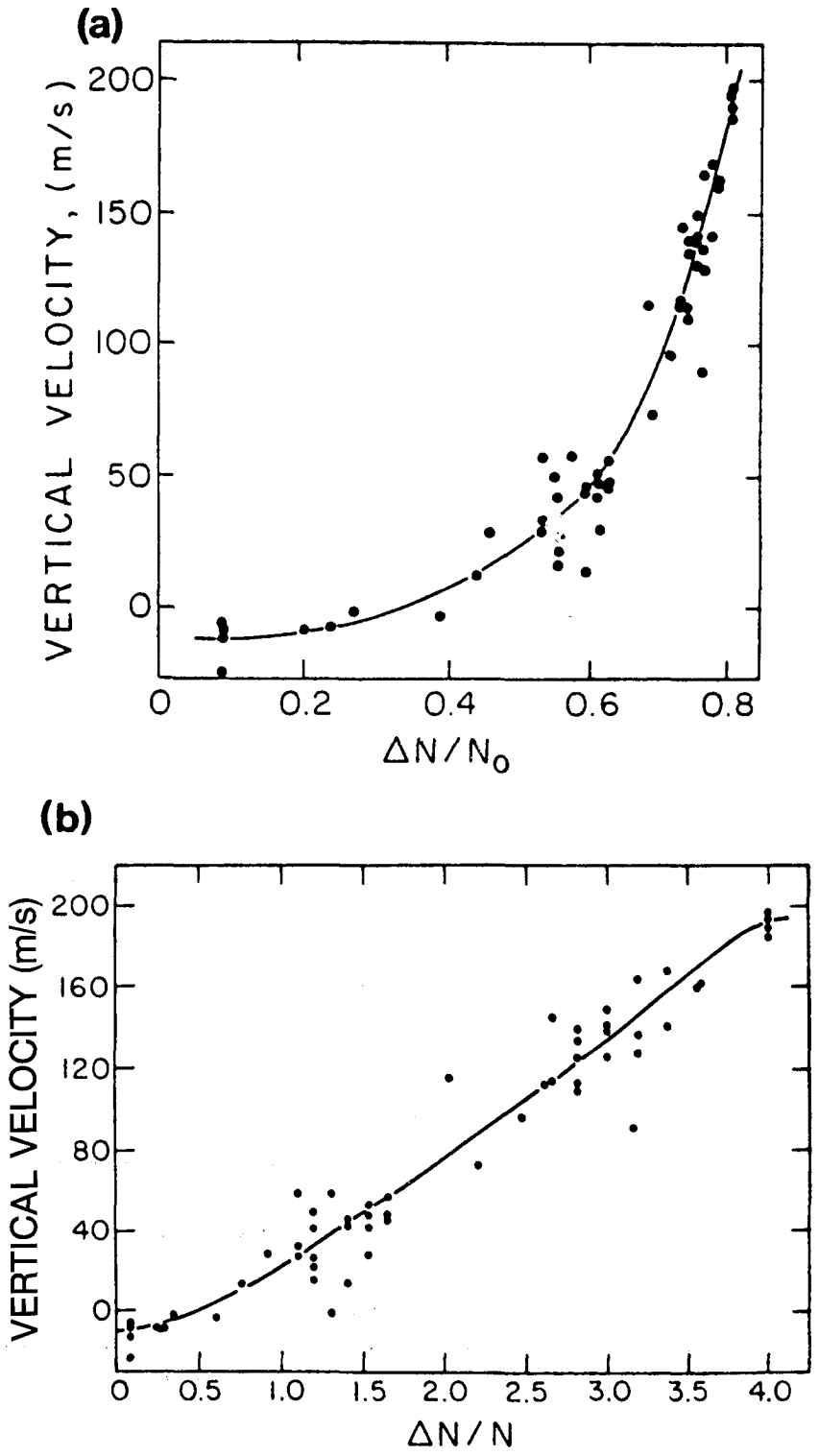


Figure 3. Vertical ion velocity data from the bubble labeled A in Figure 2 (a) plotted versus $(N_0-N)/N_0$ and (b) plotted versus $(N_0-N)/N$.

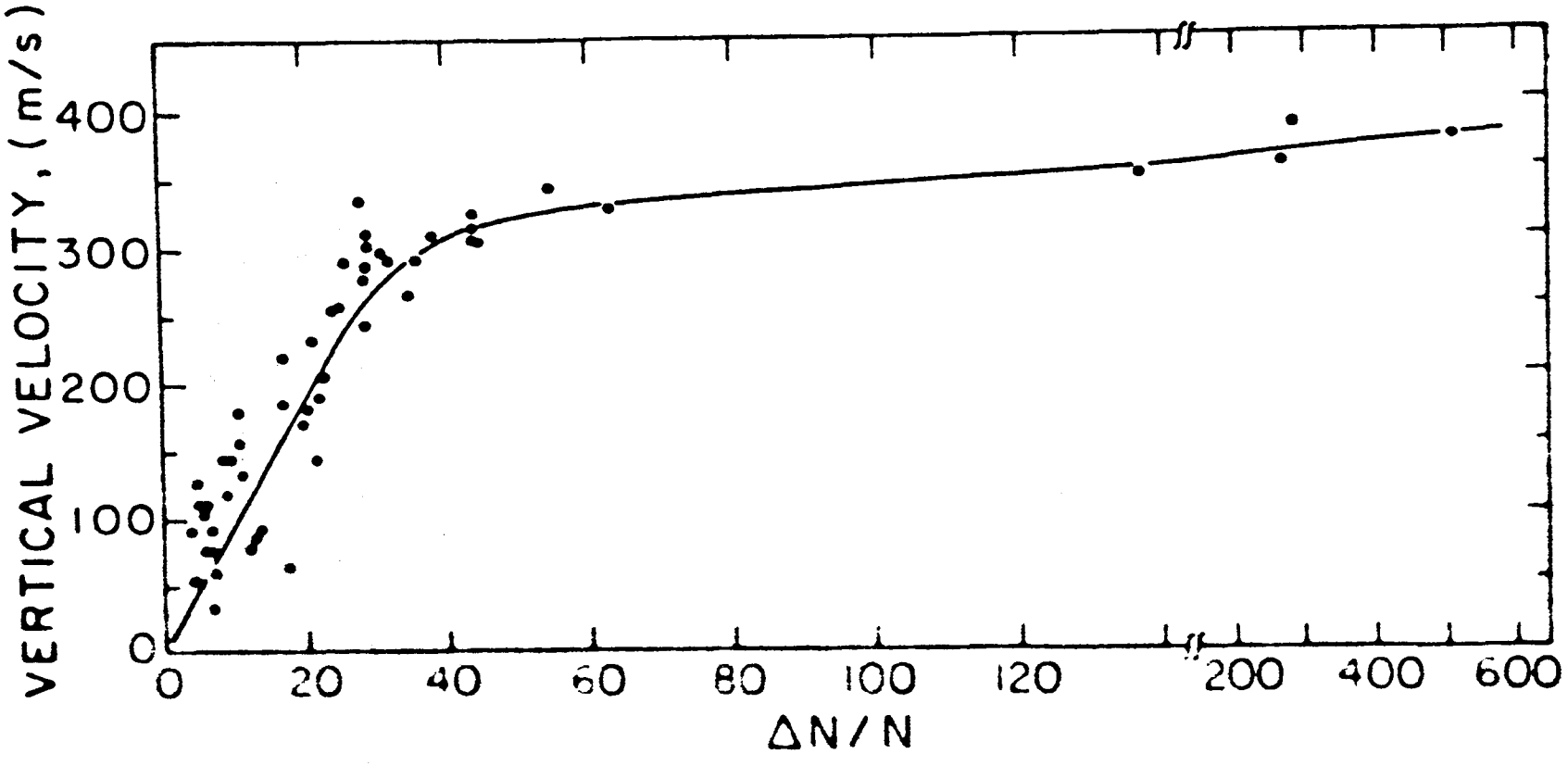


Figure 4. A plot of $V_V$ versus $(N_o-N)/N$ for one of the very low concentration bubbles of Figure 1. Note the broken scale for $\Delta N/N$.

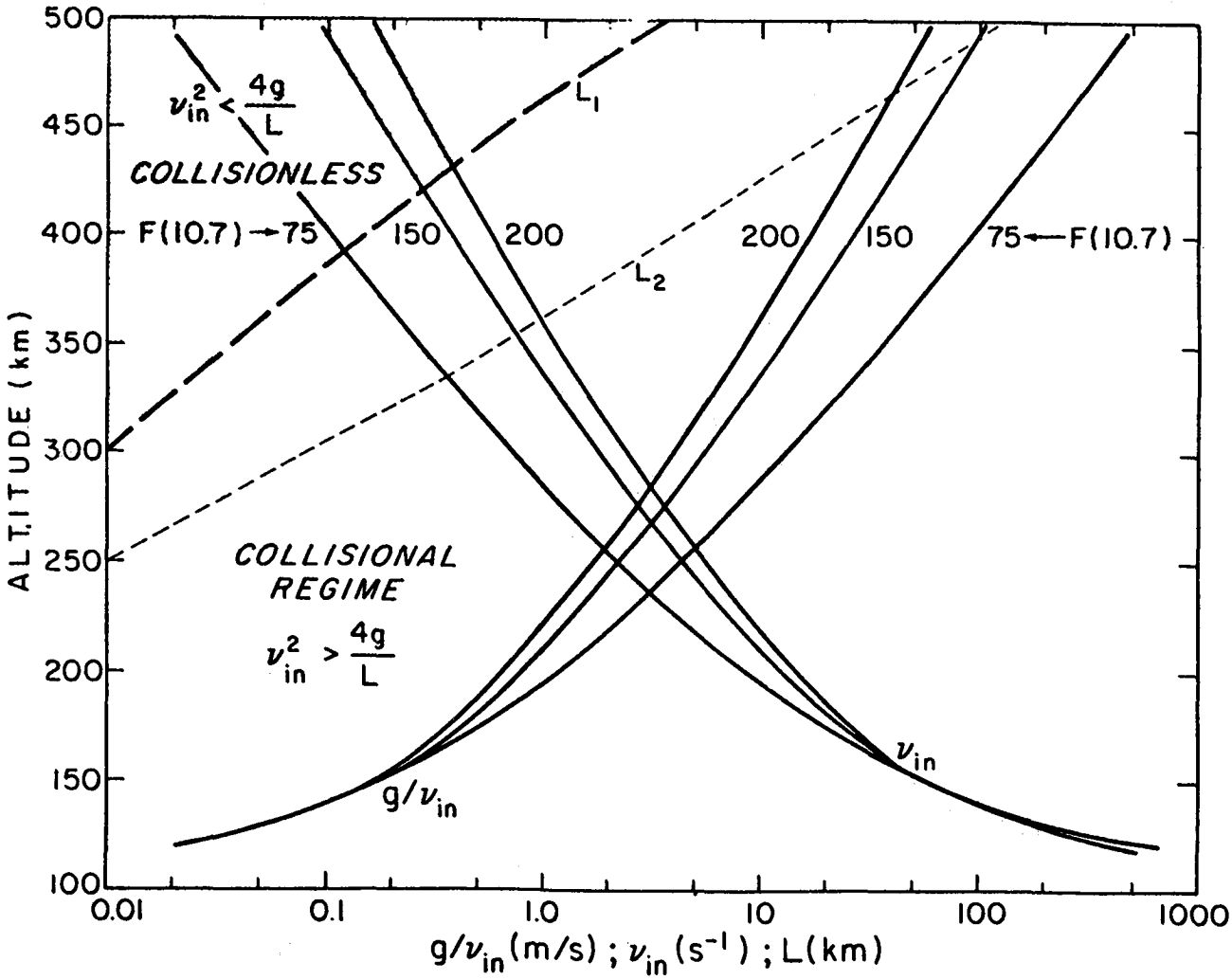


Figure 5. Plots versus altitude of the ion-neutral collision frequency ($\nu_{in}$), the ratio of gravitational acceleration to $\nu_{in}$, and the scale, L, that divides the collisional and collisionless regimes of the Rayleigh-Taylor gravitational instability. $\nu_{in}$ and $g/\nu_{in}$ are plotted for three different levels of solar activity, the MSIS model (Hedin, 1983) and collision cross sections from Banks and Kockarts (1973) were used to evaluate $\nu_{in}$. The heavy dashed line ($L_1$) defines $\nu^2_{in} = 4g/L$ for F(10.7) = 175, and the light dashed line ($L_2$) does the same for F(10.7) = 75.

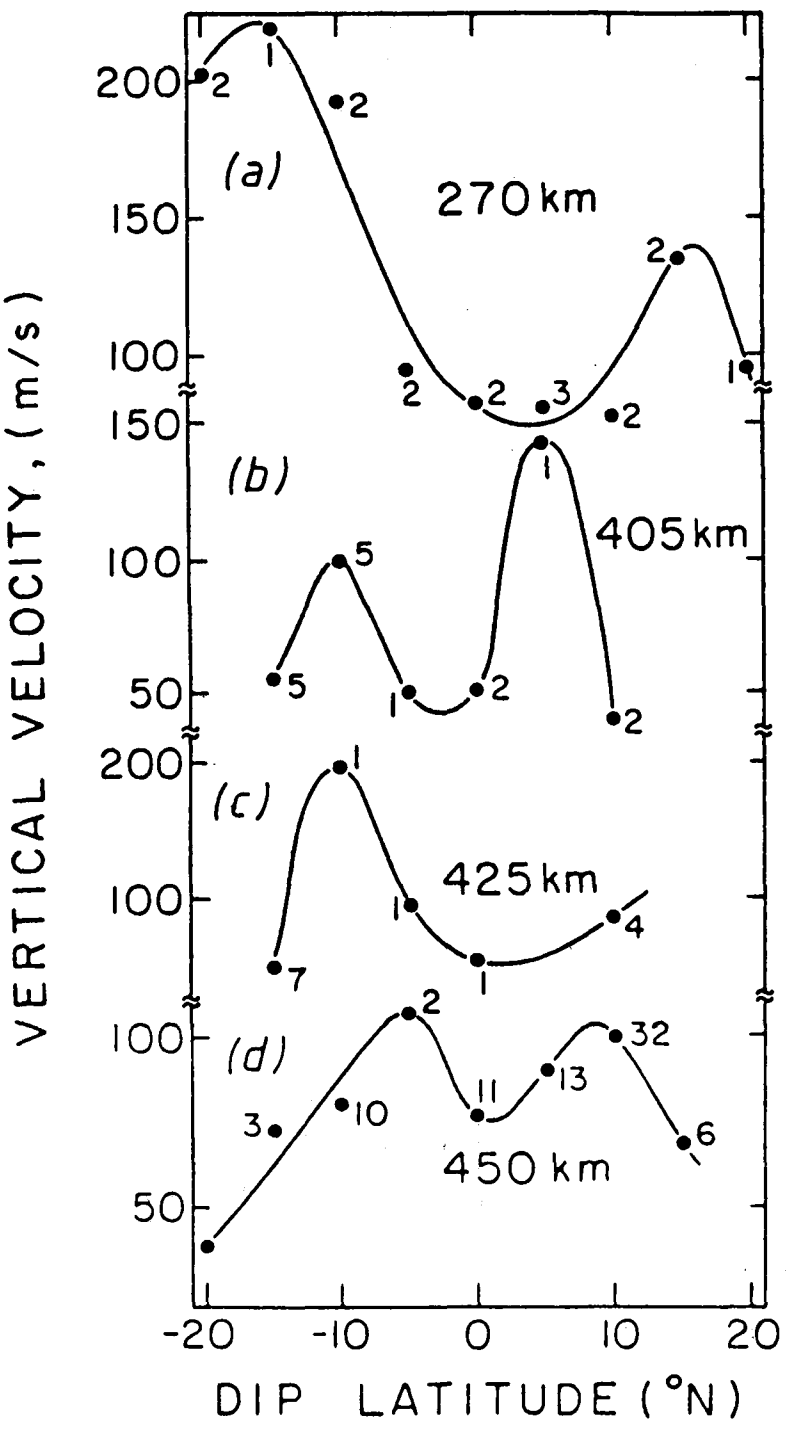


Figure 6. Vertical velocity variations with dip latitude for maximum depletions at fixed heights of 270, 405, 425, and 450 km. The number by each data point refers to the number of bubbles having that point as their mean maximum depletion velocity (low-resolution data).

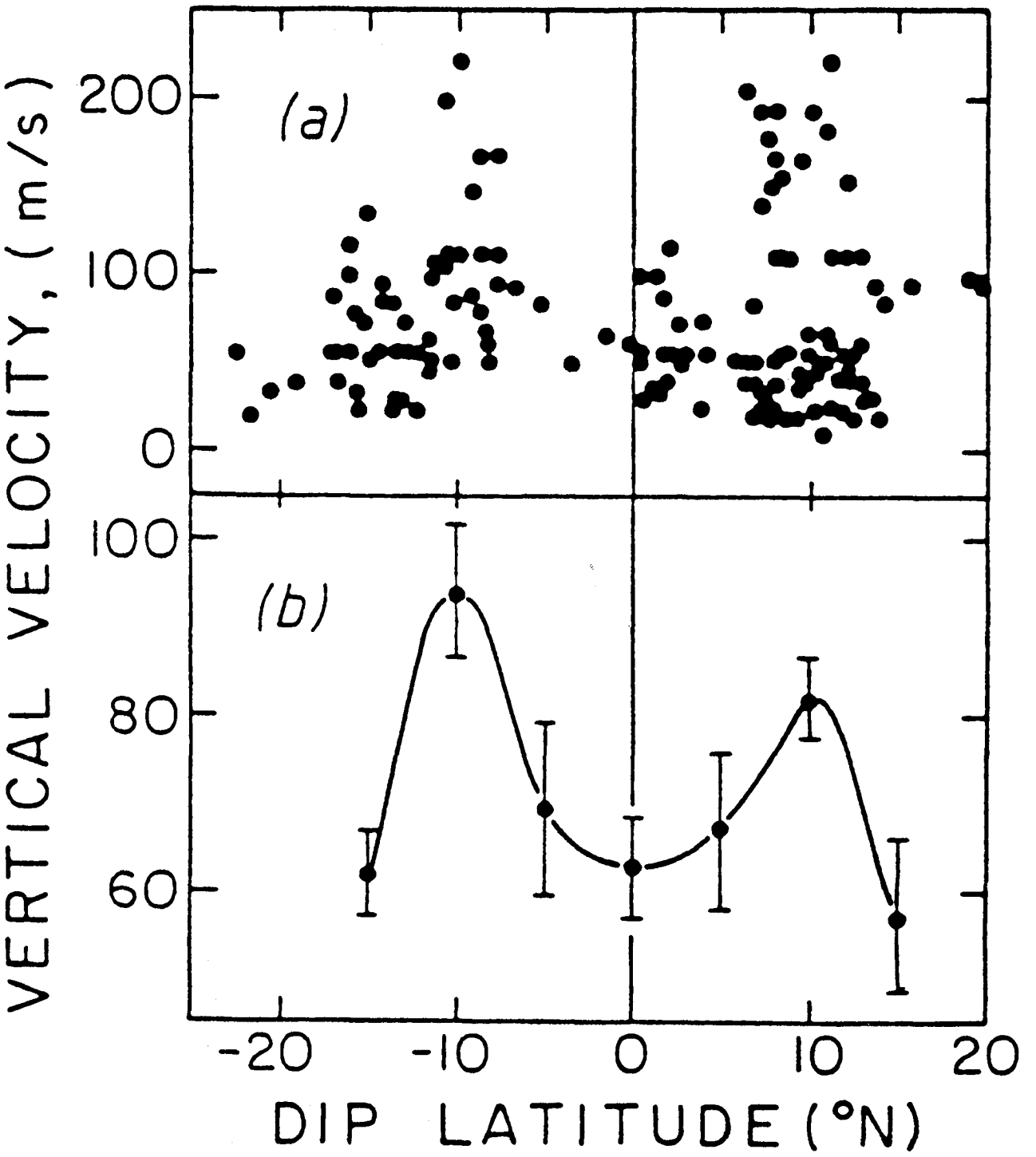


Figure 7. (a) The scatter plot and (b) the mean variation of the vertical velocity at maximum depletion as functions of dip latitude. In Figure 7b the standard error of each point is shown by a vertical bar. The data refer to bubbles with depletions of two orders of magnitude or less.

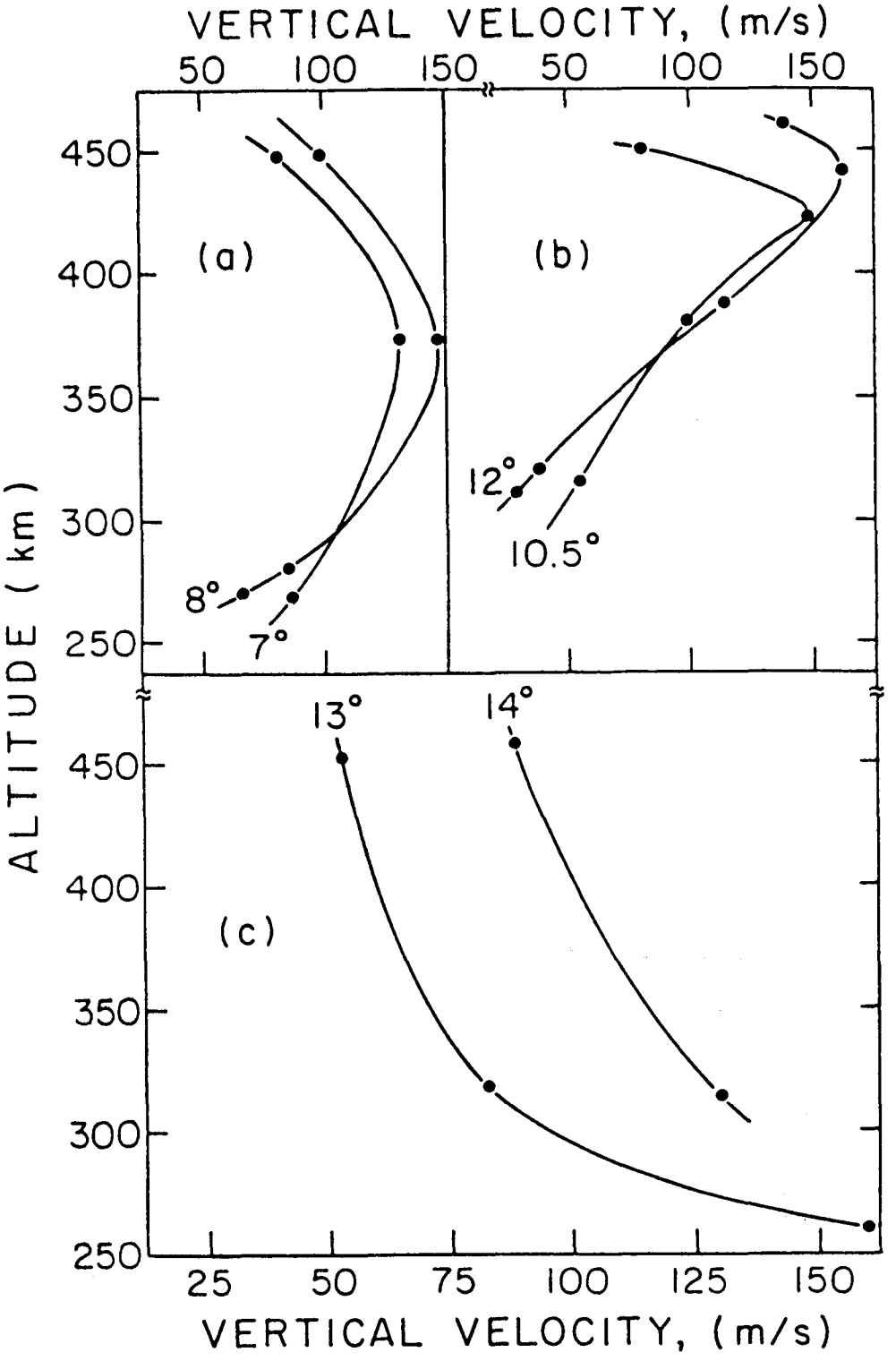


Figure 8. Variation of vertical velocity (at maximum depletion) with altitude at dip latitudes 7°, 8°, 10.5°, 12°, 13°, and 14°.

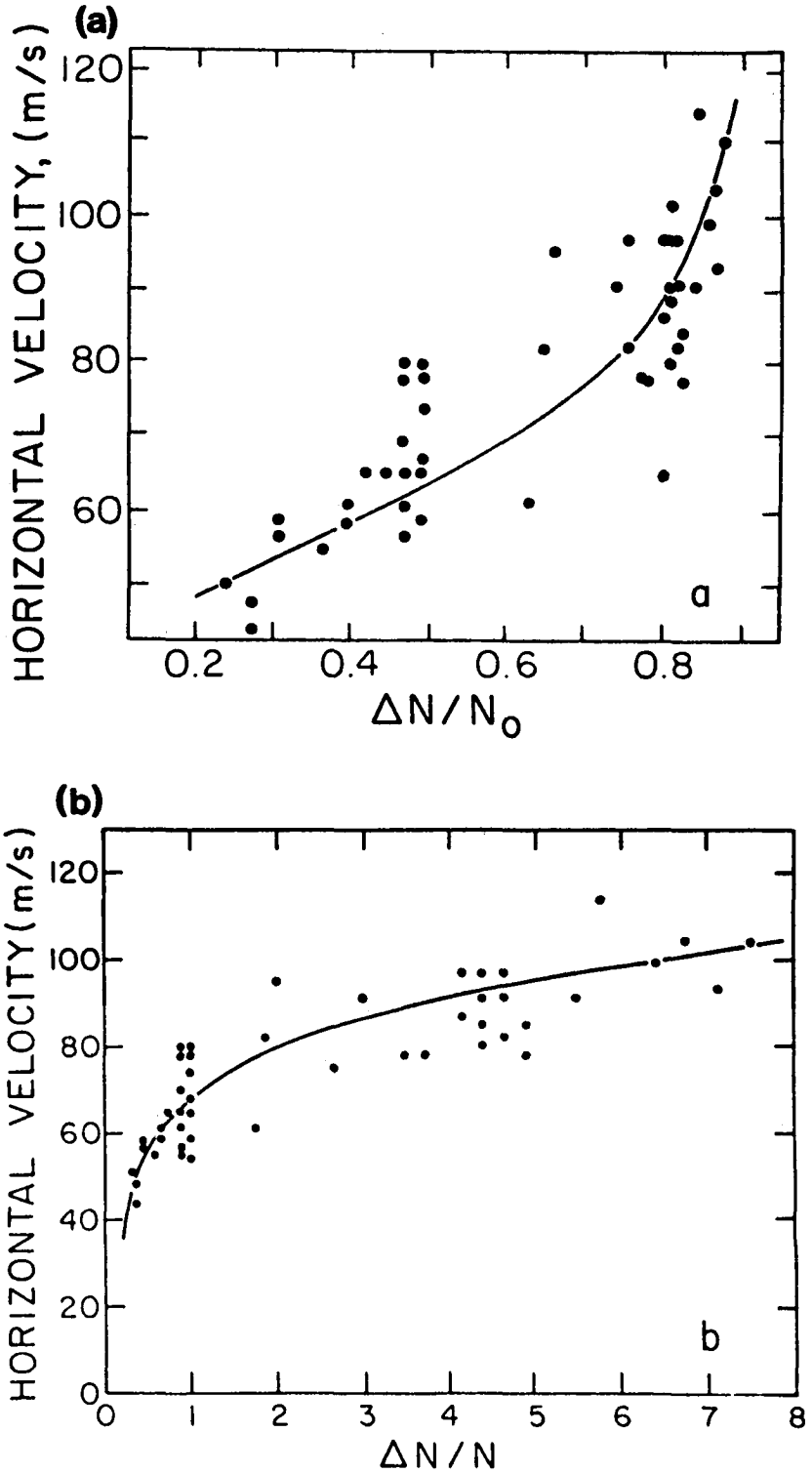


Figure 9. Plots of the horizontal ion velocity, $V_H$, versus depletion amplitude for the bubble labeled B in Figure 2. Figure 9a uses $\Delta N/N_o$ and Figure 9b uses $\Delta N/N$ for the abscissa.

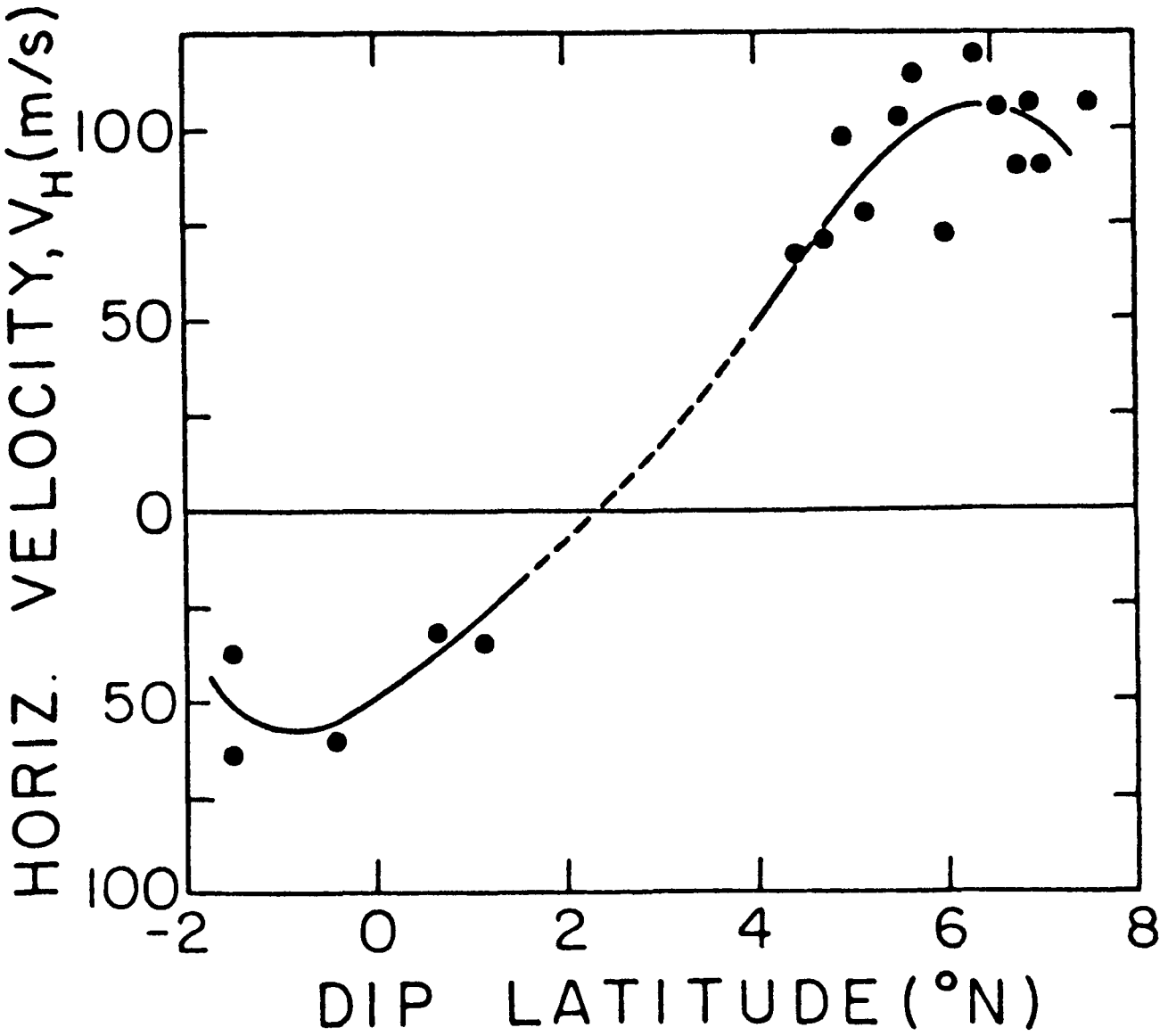


Figure 10. Plot of the maximum depletion horizontal velocity observed from the high-resolution data of AE-E orbit 20496 of July 21, 1979, as functions of dip latitude.

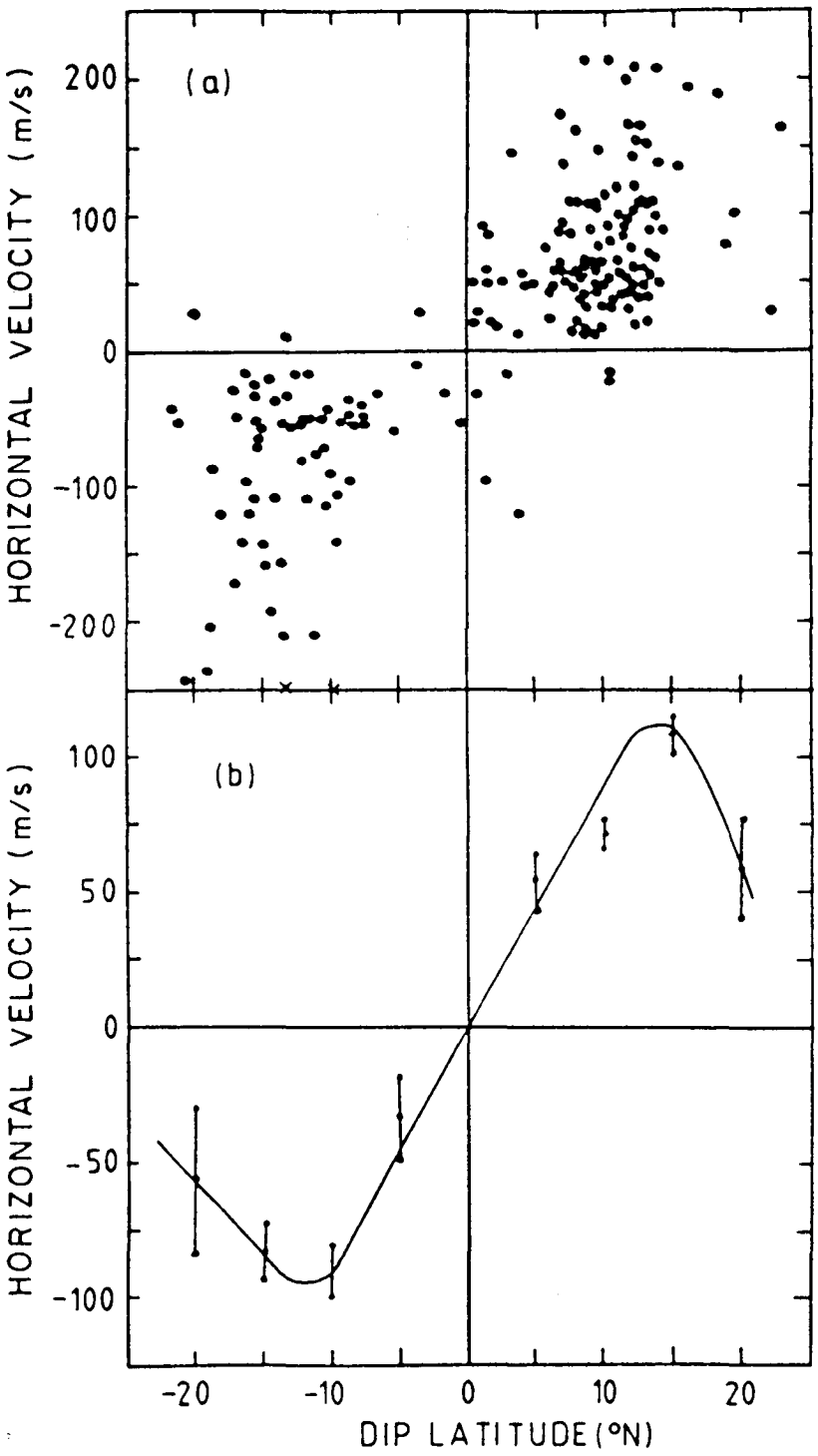


Figure 11. (a) Values of the north-south horizontal velocity at maximum depletion and (b) their mean variation, plotted as functions of dip latitude for bubbles with depletions of two orders of magnitude or less. In Figure 11b the standard error of each mean point is shown as a vertical bar.

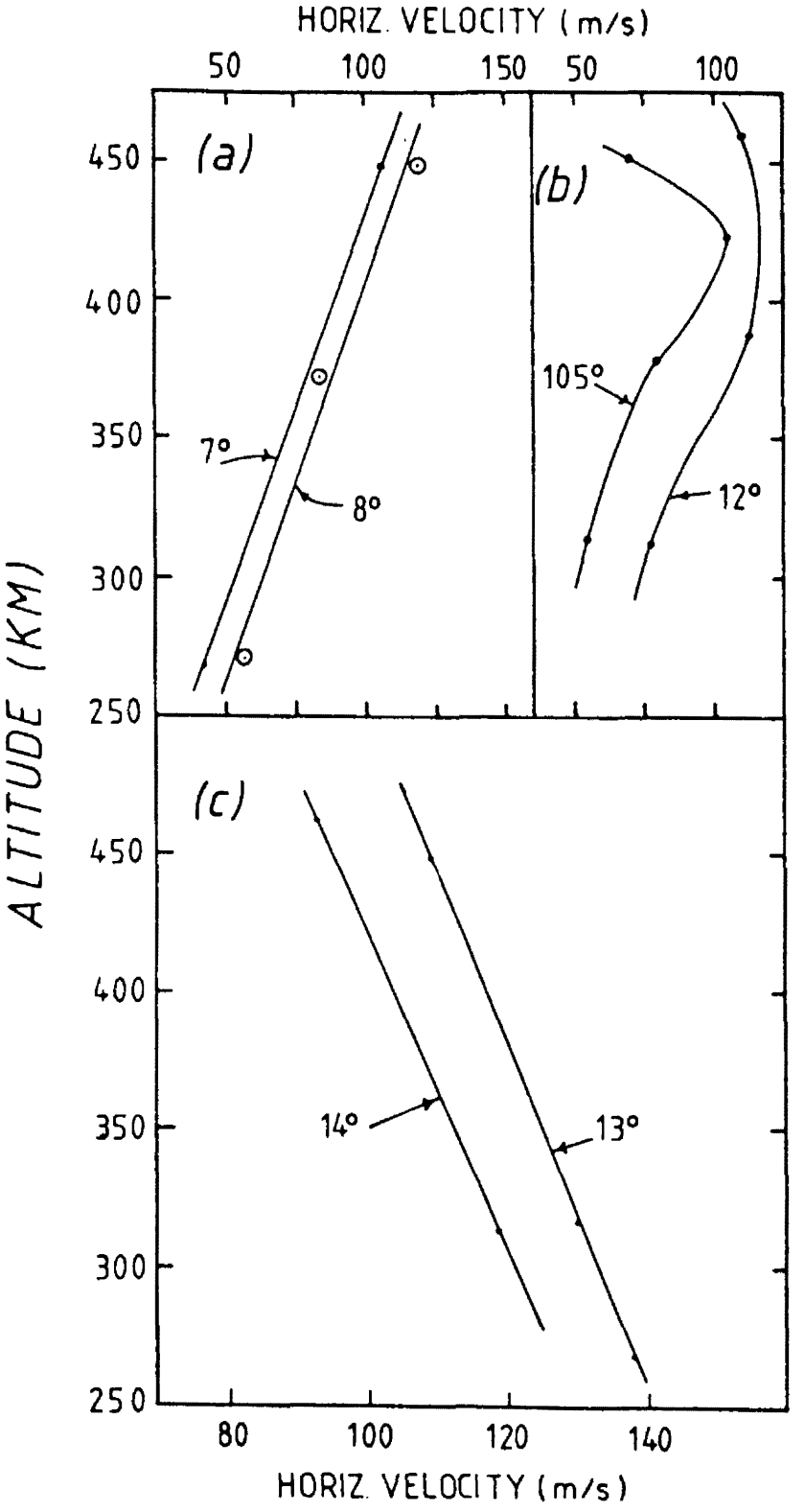


Figure 12. Same as Figure 8, but for horizontal velocity.

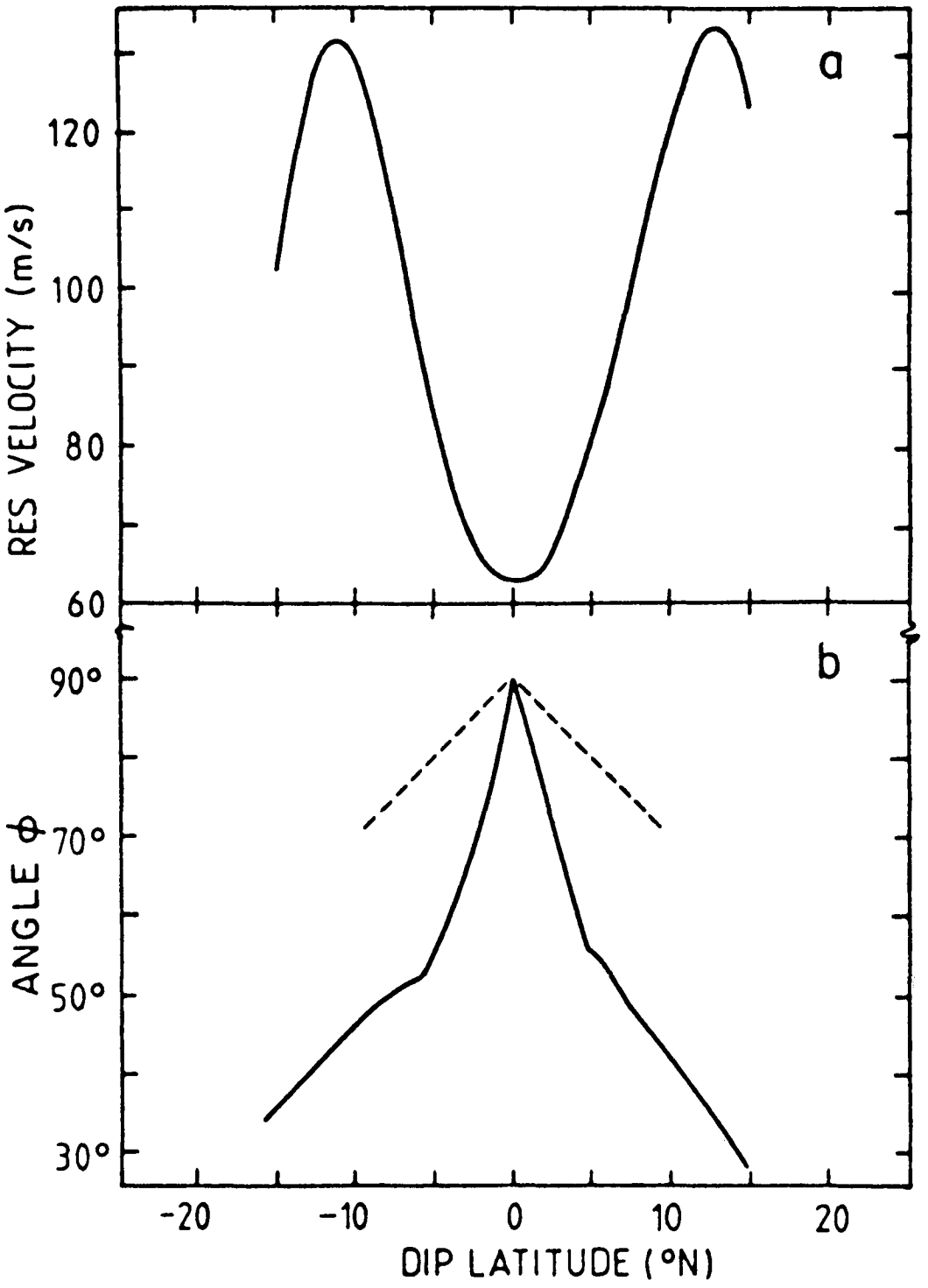


Figure 13. (a) The mean resultant ion velocity at maximum depletion as a function of dip latitude for bubbles from all the data with two-decade depletion or less. (b) The variation of the angle $\phi$ between the resultant velocity and the horizontal. The dashed lines give $\phi$ if there were no field-aligned motion.

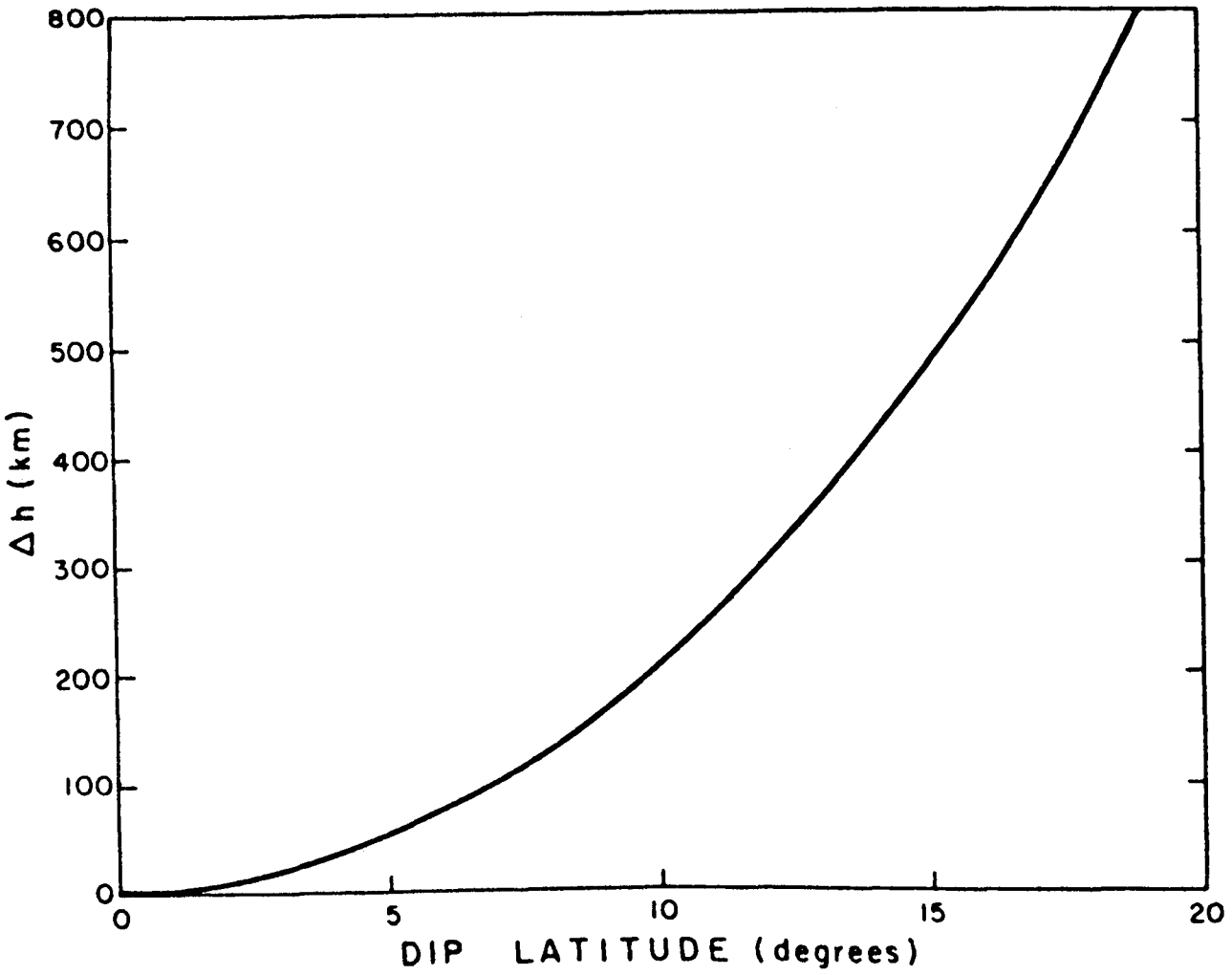


Figure 14. A plot of the altitude difference, $\Delta h$, between a satellite at radial distance $r_o$ (6700 km) and a given dip latitude to the equatorial crossing point of its dipole field line, $\Delta h = r_o \tan^2 \lambda = r_{eq} \sin^2 \lambda$.